

# The variability of rock thermal properties in sedimentary basins and the impact on temperature modelling – A Danish example

Sven Fuchs

Helmholtz Centre Potsdam, GFZ German Research Centre for Geosciences, Geothermal Energy Systems, Telegrafenberg, 14473 Potsdam, Germany



## ARTICLE INFO

### Keywords:

Well-log analysis  
Sedimentary basin  
Formation thermal conductivity  
Formation thermal diffusivity  
Formation specific heat capacity  
Formation radiogenic heat production  
Temperature modelling

## ABSTRACT

Detailed knowledge of in situ formation thermal properties is a prerequisite for accurate temperature predictions from geothermal models of sedimentary basins. The value and regional variability of such formation thermal properties generally receive little attention: very few attention in petrophysical and even less in modelling studies. Consequently, the spatial variability of formation thermal properties is typically not considered, for neither the *a priori* model parameterisation nor the *posteriori* model calibration.

This basin study determines how the thermal properties of geological formations vary spatially and how this affects the quality of modelling results compared to the results of measured temperatures in the Danish Basin. Formation petrophysical properties (thermal conductivity, radiogenic heat production, thermal diffusivity, specific heat capacity, density, and porosity) and their spatial variability in the Danish Basin are exemplarily and systematically studied by well-log interpretation techniques. Therefore, the initial computations of the mean formation well-log values (and their variability) are presented for thermal diffusivity and specific heat capacity.

The analysis reveals that all the formation thermal properties display a larger variability than previously applied in geothermal or basin modelling studies. The observed maximum variability of the mean thermal formation values is up to approximately 50% (mean:  $23 \pm 11\%$ ) for thermal conductivity, up to approximately 65% (mean:  $34 \pm 16\%$ ) for thermal diffusivity, up to approximately 30% (mean:  $16 \pm 8\%$ ) for specific heat capacity, and up to more than 100% (mean:  $64 \pm 24\%$ ) for the radiogenic heat production.

A strong regional thermal-conductivity variability impact was quantified by the comparison of subsequently modelled geotherms with measured borehole temperatures. When basin-wide mean formation conductivities (representing the usual assumption of constant formation values in geothermal models) are applied to such models, the misfit between the predicted and measured temperatures at the maximum borehole depth of approximately 4 km is large and averages approximately 20% (range:  $-21$  to  $22$  °C). Application of the observed but less representative formation conductivities in terms of the 'true' overall basin average yields maximum derivations between 27 and 66% (range:  $-38$  to  $90$  °C). The application of local formation conductivities, in contrast, yields minimum deviations generally less than  $< 5$  °C, depending on consideration of regional or location-specific heat-flow values.

Statistical data on the mean formation variability presented here can serve as guidelines to define reasonable variation ranges for the input or the post-processing calibration procedures for geothermal models of sedimentary basins with similar lithologies and genesis to the Danish Basin. In general, knowledge of the variability of formation thermal properties will lead to a significantly lower uncertainty in the temperature calculations, in particular but not exclusively for areas and depths where temperature observations are unavailable.

## 1. Introduction

In modelling the thermal fields of sedimentary basins, it is of paramount importance that the model parameterisation reflects the different rock thermal properties and their natural spatial variation in the subsurface. One of the most difficult and critical tasks is the assignment of reliable values to the different geologic units that compose

the modelled domain. In the past, the majority of numerically studied geothermal models simplified the input of thermal properties of stratigraphic units or geological formations to laterally homogeneous average values. Some exceptional modelling studies have already mentioned the importance of considering the spatial variation in thermal conductivity (e.g., Fjeldskaar et al., 2008). Recent studies, however, clearly demonstrated that considering the variability in

E-mail address: [fuchs@gfz-potsdam.de](mailto:fuchs@gfz-potsdam.de).

<https://doi.org/10.1016/j.geothermics.2018.06.006>

Received 22 February 2018; Received in revised form 25 May 2018; Accepted 20 June 2018  
0375-6505/ © 2018 Elsevier Ltd. All rights reserved.

formation thermal properties significantly and systematically reduces the difference between predicted and measured borehole temperatures (Fuchs and Balling, 2016a,b). According to a lack of properly designed petrophysical studies, the values and variability of such formation parameters are commonly unknown and thereby not considered in the pre- or post-processing of the model computation (i.e., parameterisation and calibration).

The aim of this paper is to identify and quantify the variability of petrophysical properties, in particular of thermal formation properties in sedimentary basins that are relevant for geothermal modelling. For this purpose, the variability of thermal conductivity, radiogenic heat production, thermal diffusivity, specific heat capacity, density and porosity is studied on the example of Late Permian to Cenozoic geological formations in the Danish Basin applying well-log-driven analysis techniques. The resulting impact on modelled temperature is quantified by calculating geotherms for layered thermal borehole models and varying the layer parameters within the boundaries identified by the well-log analysis. This paper provides a comprehensive study of rock thermal properties in the Danish Basin and identifies reasonable parameter variability ranges that can either be used for stochastic parameterisation and/or inverse model calibration in the Danish Basin itself or can serve as boundaries when transferred to other sedimentary basins of similar geological genesis.

## 2. Background

The thermal state and the temperature regime of the Earth's crust is mainly shaped by the basal heat flow and spatial variation in subsurface rock thermal properties. For geothermal calculations, the most important rock thermal properties are thermal conductivity (TC;  $\lambda$  in W/[m·K]), radiogenic heat production (RHP;  $A$ , in  $\mu\text{W}/\text{m}^3$ ) and the volumetric heat capacity (RHOC,  $\rho c_p$  in  $\text{kJ}/[\text{m}^3\cdot\text{K}]$ ). The latter can be described as a product of the specific heat capacity (SHC,  $c_p$  in  $\text{J}/[\text{kg}\cdot\text{K}]$ ) and density ( $\rho$  in  $\text{kg}/\text{m}^3$ ) or as a quotient of TC and thermal diffusivity (TD;  $\alpha$  in  $\cdot 10^{-6} \text{ m}^2/\text{s}$ ). While TC and RHP have a first-order effect on the terrestrial surface heat-flow density and the background steady-state temperature field, RHOC (and thereby SHC and TD) influences the transient change in heat and temperature in the crust (e.g., the paleoclimate effect, geothermal exploitation, storage of nuclear waste). As long these parameters are not well understood, accurate subsurface temperature predictions cannot be made; this is a fundamental problem for a wide range of applications (hydrocarbon maturation modelling, geothermal energy, subsurface storage of heat, nuclear waste repositories, etc.).

The spatial variation in rock thermal properties in sedimentary basins is caused by the complex interplay between the structural and lithostratigraphic, and thereby the lithofacies-dependent configuration of the geological units. Depending on the depositional environment, these changes may be random or systematic. For the TC of many lithotypes, the effect of substantial regional variations has long been known from many regional studies of well data (e.g., Chapman et al., 1984; Powell and Chapman, 1990; Deming et al., 1990; Fjeldskaar et al., 1993; Gallardo and Blackwell, 1999; Norden and Förster, 2006; Fjeldskaar et al., 2008; Fuchs and Förster, 2010; Schütz et al., 2012a,b; Norden et al., 2012; Homuth et al., 2014; Götz et al., 2014). In contrast, for TD, SHC and RHP, much less effort has been spent on similar regional well studies, although the basic interrelation of matrix minerals and pore fluid for these properties raises the expectation of a commensurate variability in sedimentary rocks and formations. However, in regard to geothermal modelling, data on the variability of thermal properties is frequently either not available or not considered as input for model parameterisation. This approach might be sufficient for the rare case of geologic formations of a uniform lithology over large distances, where it may be possible to characterize the TC from a few laboratory measurements, but this approach fails when geological formations are subject to even moderate lateral or vertical changes in

lithology (cf. Deming et al., 1990; Fuchs and Balling, 2016a).

In addition to this common negligence on the modelling side, the use of 'standard' lithotype values or laboratory measurements on material from selective borehole depths introduces further drawbacks. Upscaling from selective point data to a 'representative' mean formation value creates significant uncertainties (Fjeldskaar et al., 2008). Upscaling requires an adequate number of rock samples for laboratory studies, increasing the coring costs of a well. Even if a sufficient number of measurements are available for each rock type, it remains unclear whether the studied rock samples reflect the 'true' variation in mineralogy and petrography within the geological formation in question. As soon as the changes in rock composition between wells are taken into account, the number of measurements required increases tremendously to a number of samples generally not available without incurring the costs of numerous laboratory measurements.

An alternative to laboratory measurements is the indirect determination of rock thermal properties from geophysical well logs, which is limited to a 1D sampling volume along the borehole instead of point data in selected core sections. The well-log-based determination of rock thermal properties offers high vertical resolution and thereby a more accurate understanding of the vertical parameter distribution. A successful approach in this regards is the inversion of continuous temperature logs to borehole profiles of in situ TC (Blackwell and Steele, 1989; Fuchs and Förster, 2010; Sippel et al., 2013; Schütz et al., 2013; Fuchs et al., 2015). The computation requires stable (unperturbed) heat-flow conditions and the existence of continuous temperature logs recorded under thermal borehole equilibrium, which are very rare in most sedimentary basins. However, interpreting standard geophysical well logs is applicable far more often. For both RHP (e.g., Rybach, 1986; Bücker and Rybach, 1996) and TC (with many more methods, cf. Fuchs and Förster, 2014) this is a long-known and often-applied workflow, but only recent approaches allow the determination of TC, TD and SHC in sedimentary rocks from combinations of the most common standard log types (cf. Fuchs and Förster, 2014; Fuchs et al., 2015). However, the application of any of these well-log-driven approaches allows the calculation of reasonable mean formation values – as primarily demonstrated for inverted temperature logs by Blackwell and Steele (1989) – considering the full variability of the recorded parameter profiles and thereby the vertical changes in lithology, mineralogy and porosity. On these terms, Vogt et al. (2010) and Mottaghy et al. (2011) interpreted well logs for a TC profile and were among the first to calculate statistical values for stratigraphic units as a basis for 3D stochastic parameter realizations in a Monte-Carlo computation of a temperature model. They demonstrated that this approach is generally helpful in reducing the width (and thereby the uncertainty) of computed temperature distributions. However, as long as TC is determined at one well only, the stochastic 3D parameter distribution for each formation merely reflects the vertical variability within the formation, but not between different well locations or within a basin. When the variation in TC is also considered among different well locations in recent modelling studies, significantly lower uncertainties in temperature prediction were reported (Fuchs and Balling, 2016a,b).

Taking all these aspects into account reveals that the magnitude of variation in rock thermal properties for geological formations in sedimentary basins is often unknown but very important for the parameterisation of thermal models. Knowledge of basin-wide variations would be helpful for all geothermal numerical modelling approaches (stochastic, forward, and inverse modelling) but generally suffer from lack of data.

## 3. Geological setting and stratigraphy

The Danish Basin (DB) constitutes a major part of Denmark (Fig. 1). It is a WNW-ESE trending intracratonic basin in the eastern part of the North Sea system of sedimentary basins (Ziegler, 2005) and is bounded by the Precambrian basement blocks of the Ringkøbing-Fyn High (RFH)

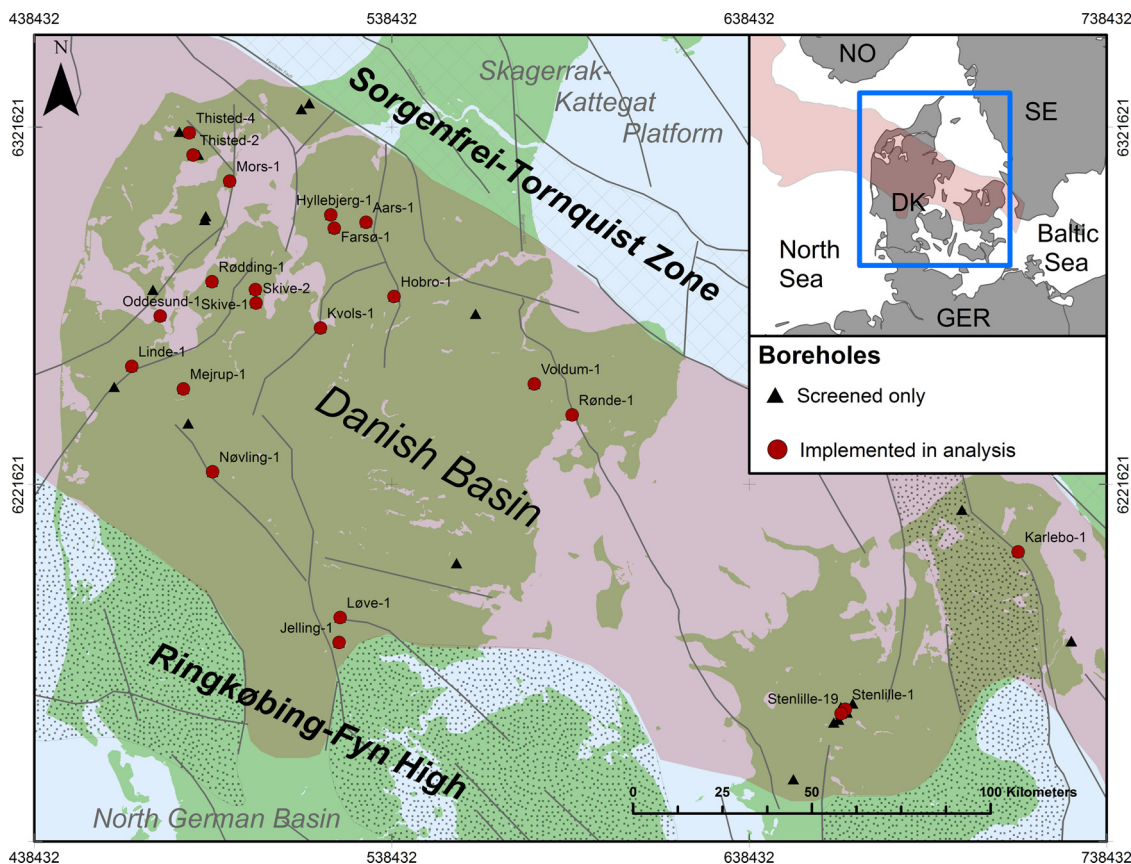


**Fig. 1.** Geological setting, main tectonic units, structural features (modified after Nielsen, 2003 and references therein), and deep boreholes located in the Danish Basin (cf. Appendix A). Pink shaded: Danish Basin; grey lines: major faults. Abbreviations: DK = Denmark, NO = Norway, SE = Sweden, GER = Germany. Model coordinates are given in a UTM (zone 32 N) system using the WGS 84 datum (For interpretation of the references to color in this figure legend, the reader is referred to the web version of this article).

towards the southwest and by the Fennoscandian Border Zone including Skagerrak-Kattegat Platform (SKP) and the (block faulted transition zone) Sorgenfrei-Tornquist Zone (STZ) towards the north-east (Sorgenfrei and Buch, 1964; Bergström, 1984; EUGENO-S Working Group, 1988). The DB is synonymously named the Danish part of the Norwegian–Danish Basin (Bertelsen, 1978; Michelsen, 1978).

The sedimentary sequence (Fig. 2) and the structural framework of the Danish Basin are well known from seismic investigations and several oil and gas exploration boreholes. The DB is a Late Carboniferous–Permian to Cenozoic structure and was formed by Late Palaeozoic and Triassic lithospheric extension and thermal subsidence between the Skagerrak-Kattegat Platform and the Ringkøbing-Fyn High (Vejbæk, 1989; Frederiksen et al., 2001). The subsidence was balanced by the deposition of sediments mainly from the northern boundary, resulting in a basin that consists of up to 5–10 km of Permian, Mesozoic and Cenozoic sediments with the deepest areas in the north-western parts of the basin (Hamberg and Nielsen, 2000; EUGENO-S Working Group, 1988). The DB is characterized by thick Triassic units (up to 4–6 km of mainly silt and sandstone) and moderately thick units of Upper Cretaceous carbonates (1–2 km of chalk and limestone). More locally, Jurassic to Lower Cretaceous claystone of up to 1.5 km may be present (Bertelsen, 1980; Michelsen and Clausen, 2002; Michelsen et al., 2003; Nielsen, 2003). The Zechstein salt forms the source of significant tectonic salt uplifting and diapirism, in particular in the north-western (onshore) part of the basin. Major regional aquifer systems with high geothermal energy potential were identified (e.g., Mathiesen et al., 2009, 2010), in particular in the Jurassic and Triassic sequence. The most promising reservoirs are the Upper Jurassic Frederikshavn Member, the Middle Jurassic Haldager Sandstone Member, the Lower Jurassic Gassum Formation, and the Triassic Bunter Sandstone and

Skagerrak Formations. These formations were the target for extensive investigations of geometrical distribution and petrophysical properties (e.g., Hamberg and Nielsen, 2000; Nielsen, 2003; Weibel et al., 2011, 2017).

The RFH to the south of the DB is a NW-SE trending basement ridge that separated the Southern Permian Basin from the Northern Permian Basin during Late Carboniferous to Early Permian times. It consists of a series of shallow fault-bounded crystalline blocks of Precambrian age (spanning between the North Sea and the Baltic Sea) and it is separated by the N–S striking Brande and Horn Graben. These Graben systems were generated during the Late Carboniferous to Early Permian by movements along the Sorgenfrei-Tornquist Zone and the Trans European Suture Zone (Thybo, 1997, 2001; Bergerat et al., 2007; Sorgenfrei and Buch, 1964). The subsequent progressive uplift of the Ringkøbing-Fyn High was associated with the Early Middle Jurassic major updoming of the North Sea area (Ziegler, 2005). In contrast to the DB, only thin sections of Triassic to Lower Cretaceous sediments are present above the RFH (Nielsen, 2003).

## 4. Analysis

### 4.1. Data

This study benefits from a large amount of borehole data from 56 deep wells in the study area provided by the Geological Survey of Denmark and Greenland (GEUS). The studied boreholes reach depths between 909 and 5303 m below sea level (mbsl) (28 out of the 56 wells reach depths > 2000 mbsl). Geological, geophysical and final well reports as well as geological, petrophysical and well-log data were screened to select boreholes with high-quality data, resulting in a final

| System     | Stage                      | Danish Basin                   |         | Main lithology   |
|------------|----------------------------|--------------------------------|---------|--|
|            |                            | NW                             | SE      |  |
| Cenozoic   | Danian                     | Post Chalk Group               | unit 1  | sand, silt, clay                                       |
|            | Maastrichtian - Cenomanian | Chalk Group                    | unit 2  | carbonate rocks  |
| Cretaceous | Albian - Berriasian        | Rødby Fm. / Veldsted Formation | unit 3  | mudstones  |
|            | Volgian                    | Frederikshavn Formation        | unit 4  | siltst., fine-grained sandst. interb. clayst.          |
| Jurassic   | Upper Kimmeridgian         | Børgelum Formation             | unit 5  | slightly calcareous claystones, mudstones              |
|            | Oxfordian                  | Flyvbjerg Formation            | unit 6  | siltstones and fine-grained sandstones                 |
|            | Middle Callovian           | Haldager Sand Formation        | unit 7  | sandstones, thin siltstone, claystone and coal beds    |
|            | Bathonian                  |                                |         |  |
|            | Bajocian                   |                                |         |  |
|            | Aalenian                   |                                |         |  |
|            | Lower Toarcian             | Fjerritslev Formation          | unit 8  | slightly calcareous claystones, with siltstone laminae |
|            | Pliensbachian              |                                |         |  |
|            | Sinemurian                 |                                |         |  |
| Hettangian |                            |                                |         |  |
| Triassic   | Upper Rhaetian             | Gassum Formation               | unit 9  | sandstones interbedded with claystones                 |
|            | Norian                     | Vinding Formation              | unit 10 | clayst., marls, oolitic carbon.                        |
|            | Carnian                    | Oddeund Formation              | unit 11 | clayst. and siltst., interbed. dol. limest.            |
|            | Ladinian                   | Tønder Formation               | unit 12 |  |
|            | Middle Anisian             | Falster Formation              | unit 13 | limestones, claystones and halites                     |
|            | Olenikian                  | Ørslev Fm.                     | unit 14 | sediments, halite, anhydrite                           |
|            | Lower Jakutian             | Bunter Sandst. Fm.             | unit 15 | sandstone interb. with mudstones                       |
|            | Brahmanian                 | Bunter Shale                   | unit 16 | claystones   |
| Permian    | Changhsingian              | Zechstein Group                | unit 17 | evaporite rocks, mainly rock                           |
|            | Wuchiapingian              |                                |         |  |

Fig. 2. Stratigraphic table, geological formations and generalized lithology for the Danish Basin (modified after Bertelsen, 1980; Michelsen and Clausen, 2002; Michelsen et al., 2003; Nielsen, 2003; Nielsen et al., 2004); colours – blue: carbonate dominated, yellow: sandstone dominated, grey: clay-/mudstone dominated, brownish: no dominant lithology, lilac: evaporites (For interpretation of the references to color in this figure legend, the reader is referred to the web version of this article).

data set of 23 wells for the DB. For each of these wells, mainly drilled for oil and gas exploration between 1951 and 2011, lithologic and stratigraphic information, digital log data and test data (e.g., drill stem tests) were implemented in the analysis. Logging data in the selected wells cover a broad spectrum of standard well logs (usually resistivity, self-potential, gamma-ray and spectral gamma-ray log, density log, sonic log, neutron log, photoelectric factor, and caliper log). All logging data were re-sampled to fixed 0.25-m intervals and corrected for borehole or environmental effects (compensated logs), in particular considering the effects of drilling muds and borehole breakouts, following procedures documented by Serra (1986) and Theys (1999).

#### 4.2. Workflow and methods

The analysis conducted consists of two steps. In the first step, profiles of the bulk (considering the sum effect of matrix and pore-filling fluid) TC, SHC, and TD are calculated for each borehole by applying the prediction equations for sedimentary rocks developed by Fuchs et al. (2015). These equations were developed on a slightly modified Fuchs and Förster (2014) concept and allow the estimation of rock thermal properties (TC, TD and SHC) for each combination of up to five standard well logs and derived predictors (the volume fraction of shale: VSH [-], interval sonic transit time: DT [μs/m], neutron porosity: NPHI [-], bulk density: RHOB [g/cm<sup>3</sup>], and photoelectric factor: PE [-]). To minimize the expected prediction error along the borehole, only equations with at least three predictor variables are applied, depending on the depth-specific major sedimentary rock group (carbonates, clastic rocks, evaporites) and the available well-log combination (mainly combinations of DT, RHOB, VSH and/or NPHI). Consequently, Eqs. (11)–(15); 31–46, and 62–77 from Appendices A–C of Fuchs et al. (2015) are implemented in the analysis.

Profiles of radiogenic heat production (RHP) are either calculated from the uranium, thorium and potassium concentrations detected by the spectral gamma ray and the logged density (Eq. (1)) or, where only standard gamma-ray readings (γ) are available, from an empirical equation for this parameter (Eq. (2)) (Rybach, 1986; Bücker and Rybach, 1996). Both methods allow the determination of RHP [μW/m<sup>3</sup>] with an uncertainty typically lower than 10% when applied to a carefully processed log data set.

$$A = 10^{-5} \rho (9.52 c_u + 2.56 c_{Th} + 3.48 c_K) \tag{1}$$

$$A = 0.0145 \cdot (\gamma - 5) \tag{2}$$

The volume fraction of shale (VSH) encompasses all clay minerals and is determined from the GR log and basically approximated as the gamma-ray index (VSH = GRI, for laminated shales) from the gamma-ray readings (Serra, 1986):

$$V_{sh} = GRI = \frac{\gamma - \gamma_{min}}{\gamma_{max} - \gamma_{min}} \tag{3}$$

Therein, γ is the gamma-log reading at the point of interest [in API units], γ<sub>min</sub> is the clay-free log reading (clean sandstone line), and γ<sub>max</sub> is the pure-clay reading (shale baseline). In young rocks (Quaternary and Tertiary rocks), the shale model that is a non-linear function of GRI and that was proposed by Clavier et al. (1971) is additionally applied:

$$V_{sh,Clavier} = 1.7 \sqrt{3.38 - (GRI + 0.7)^2} \tag{4}$$

Porosity is estimated from compensated sonic, density and neutron logs by applying standard well-log processing techniques (Serra, 1986). Sonic porosity is calculated from both the time-averaged equation (Eq. (5)) proposed by Wyllie et al. (1958) and the Raymer-Hunt-Gardner

equations (Eq. (6); Raymer et al., 1980). Therein, for example, compressional matrix transit times of 161  $\mu\text{s}/\text{m}$  (limestone) and 184  $\mu\text{s}/\text{m}$  (sandstone), and compressional fluid transit times of 620  $\mu\text{s}/\text{m}$  are used. Values for other rock types used in this analysis are documented by Serra (1986; p. 74). The appropriate lithology is determined by cross-plot and layover techniques from well logs.

$$\phi_s = \frac{\Delta t - \Delta t_{ma}}{\Delta t_{fl} - \Delta t_{ma}} \frac{1}{C_p} \quad (5)$$

$$\phi_{rhg} = (5/8) \cdot (\Delta t - \Delta t_{ma}) / \Delta t \quad (6)$$

Total porosity is calculated primarily as density-neutron average porosity (in limestone units) that is largely free of lithology effects; otherwise, sonic porosity is used. In a final step, for each borehole, all depth intervals with parameter determinations are merged to the best prediction profiles for TC, TD, SHC, RHP, and, if applicable, density and porosity. For computation of the mean formation values, the application of the arithmetic mean is equal to the lithological-thickness weighted arithmetic mean since all well-log data are sampled at regular intervals of 0.25 m. The mean variability of formation (FM) values are computed as:

$$\text{Variability} = 0.5(FM_{\max} - FM_{\min}) / FM_{\text{basin}} \quad (7)$$

where  $FM_{\max}$  is the maximum mean formation value,  $FM_{\min}$  is the minimum mean formation value and  $FM_{\text{basin}}$  is the overall mean formation value in the basin.

In the second step, the effect of the observed basin-wide TC variation on the subsurface temperature is quantified by calculating 1D steady-state geotherms for the example of three well locations. By applying a bootstrapping method, the basal temperature  $T_B$  of a rock layer with thickness  $\Delta z$  can be calculated under 1D steady-state conductive conditions from the temperature ( $T_T$ ) and heat flow ( $q_T$ ) at the top of the layer, considering the thermal properties ( $k$ ,  $A$ ) of the layer:

$$T_B = T_T + \frac{q_T}{k} \Delta z - \frac{A \Delta z^2}{2k} \quad (8)$$

The heat flow at the top of the layer thereby decreases with depth according to:

$$q_T = q_B + A \Delta z \quad (9)$$

By application to successive layers, geotherms are calculated from the surface to depth. The layer thickness is set to 1 m. The selected wells cover a depth range between 1.6 and 5.2 km and serve as examples for the large variation in thickness, depth and rock type occurring in different Late Permian to Cenozoic formations. This configuration should allow one to roughly quantify whether neglecting the lateral variation in rock thermal properties by setting a location-specific parameter as the representative for a basin-wide homogenous parameterisation of geological formations results in substantially larger uncertainties of predicted temperatures.

The heat-flow value overprint of the long-term ground surface temperature history needs to be taken into account as model input for the Northern Hemisphere. It is well known that several glaciations took place in Denmark, resulting in transient thermal effects and perturbations of the subsurface temperatures and heat-flow field (cf. Fjeldskaar and Amantov, 2017). Several studies addressed this issue for the Danish region (e.g., Balling, 1986; Balling et al., 1992). Most recently, Balling (2013) compiled heat-flow data from wells and several depth sections across Denmark and showed the variation with depth caused by glaciation. The data from Balling (2013, Fig. 5.9,  $n = 44$  values) were determined from core and partly log measurements and temperature data in nine boreholes between the surface and a depth of 2.5 km, whereas the majority are clustered in the upper 1.5 km. The observed heat-flow range above 500 m is between approximately 30 and 40  $\text{mW}/\text{m}^2$ , and increases to between 70 and 75  $\text{mW}/\text{m}^2$  below 2000 m. From these data, a polynomial equation was computed and implemented as a

heat-flow function generalized for the Danish region in the 1D steady-state conductive models:

$$q_T = 2.183[(\cdot 10)]^{-12} D^4 - 1.839 \cdot [(10)]^{-8} D^3 + 4.230 \cdot [(10)]^{-5} D^2 - 7.852 \cdot [(10)]^{-3} D + 3.282 \quad (10)$$

This formulation describes the original dataset (depth  $[D]$  in  $m$ ) range: 0–2500 m) with an uncertainty range of approximately  $\pm 5 \text{ mW}/\text{m}^2$  at any depth. For locations A (Aars) and B (Stenlille), site-specific heat-flow densities are computed in addition (Balling et al., in preparation), based on continuous TC profiles that are validated on core measurements (data taken from Balling et al., 1981) and continuous temperature gradient profiles. From there, additional geotherms are computed to compare the impact of knowing local heat-flow data with the application of the generalized heat-flow-depth relation.

### 4.3. Statistics

For each geological formation, the mean values (thickness weighted arithmetic mean and median), standard deviation (1-sigma), 95% confidence interval of the mean, quartiles (min,  $Q_{0.25}$ , median,  $Q_{0.75}$ , max) and number of log data points ( $n$ ) are calculated. Calculations are performed separately for each borehole and for the whole study area. Deviations between computed geotherms and measured temperatures are calculated, using the arithmetic mean error (ame), 1-sigma standard deviation (sd), median and root mean square error (rmse). A comparison of formation mean values is performed using the student's  $t$ -test for unpaired samples. For statistical significance, a level of 5% ( $\alpha = 0.05$ ) is chosen as the threshold. For  $p$  values  $< \alpha$ , the null hypothesis (mean formation values are equal) is rejected in favour of the alternative hypothesis (mean formation values are significantly different). Compared groups have been initially tested for normal distribution using the Kolmogorov–Smirnov test and for equality of variances using the Levene test. More details on the applied statistical computations are documented by Deutsch and Journal (1998).

## 5. Results

The main goal is to identify the variability of rock thermal properties in sedimentary formations across the Danish Basin using well logs from boreholes and to quantify its effect on subsurface temperature modelling (Section 6.3). To distinguish real regional variation in the mean well-log values of geological formations (Section 6.2) from small discrepancies of the applied interpretation methods, one needs to quantify the uncertainties of the applied well-log-based prediction approach (Section 6.1). In addition to the equation-specific uncertainties, this is of particular importance as I used varying well-log combinations, and thus varying prediction equations and correspondingly varying uncertainties.

### 5.1. Quantification of prediction uncertainties

An example of the well-log-based prediction of TC, TD and SHC is illustrated in Fig. 3, including the associated variations in the predictions. It shows that large vertical variations in rock thermal properties can be observed both within and across geological formations, as well as that when the single equations are applied for all possible combinations of well logs, it mostly results in predicted profiles with a similar form and relatively small deviations. Along the borehole, the span between the minimum or maximum profile and the mean of all predicted profiles is  $0.23 \pm 0.12 \text{ W}/(\text{m}\cdot\text{K})$  [ $10.1 \pm 5.5\%$ ] for TC,  $0.10 \pm 0.06 \cdot 10^{-6} \text{ m}^2/\text{s}$  [ $12.5 \pm 8.3\%$ ] for TD, and  $102 \pm 54 \text{ J}/(\text{kg}\cdot\text{K})$  [ $6.8 \pm 3.5\%$ ] for SHC. As a kind of validation, bulk density is calculated (Fig. 3; right panel) from the predicted thermal-rock-property profiles (equation:  $\rho_b = \lambda/c_p \alpha$ ) and compared to the logged bulk density. Good agreement is observed between the profiles, showing



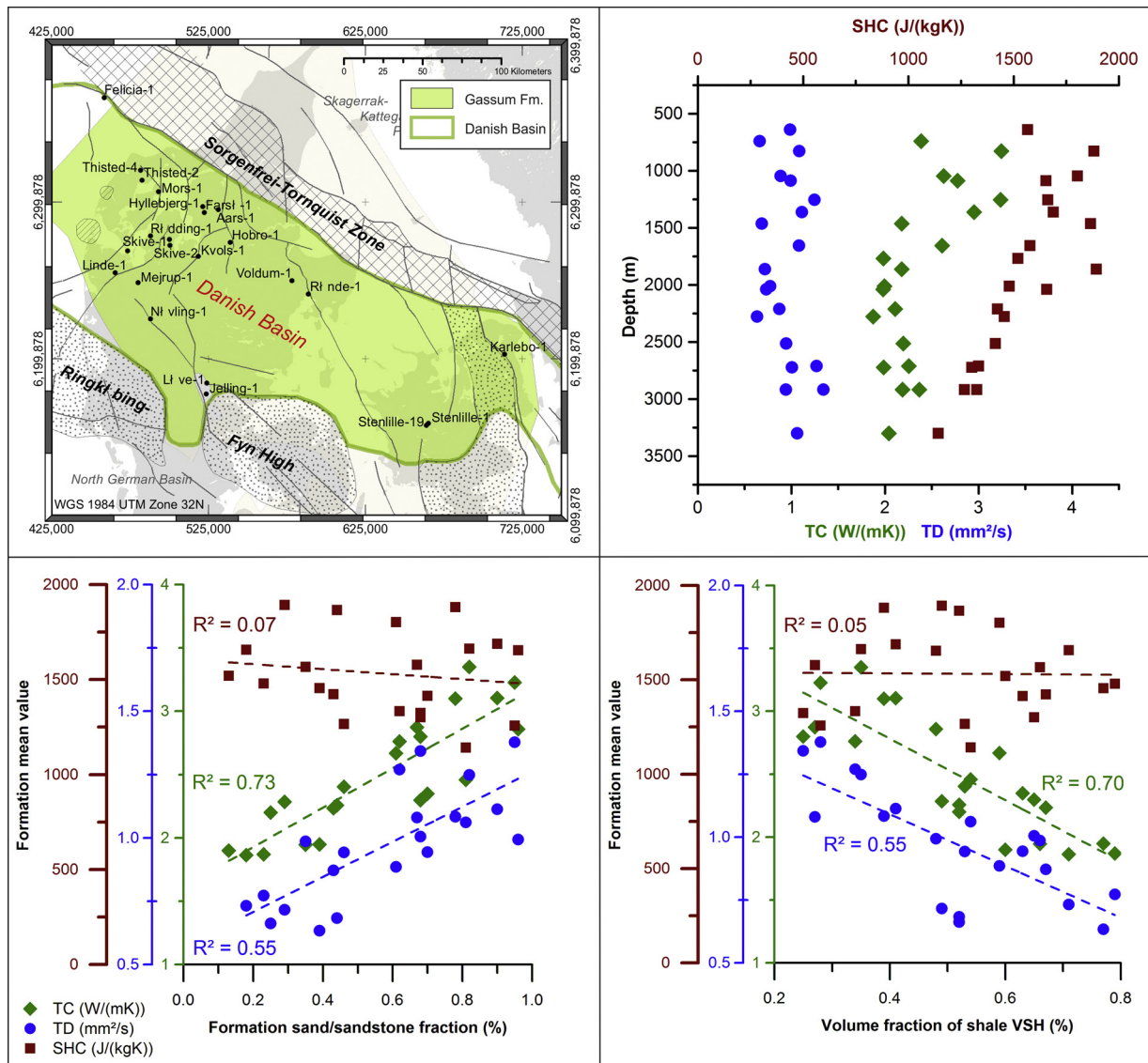


Fig. 5. Well-specific mean formation values of thermal conductivity, thermal diffusivity, and specific heat capacity of the Gassum Formation versus depth (top right), formation sandstone fraction (bottom left), and volume fraction of shale (bottom right).

$\phi$ ,  $\rho_b$ ) for the geological formation intervals allows one to observe the lateral variability from well to well within a basin. (Fig. 6). The statistical results of the illustrated thermal and additional petrophysical properties (density and porosity) are reported in Table 1. Formation TC values mainly range between 1.7 W/(m K) and 4.4 W/(m K), except for the Zechstein Formation that generally exhibits higher values, mainly between 3.2 and 4.9 W/(m K). Likewise, TD mainly ranges from approximately 0.3 to  $1.7 \cdot 10^{-6} \text{ m}^2/\text{s}$  for clastic or carbonaceous formations and from  $1.4$  to  $2.8 \cdot 10^{-6} \text{ m}^2/\text{s}$  for the Zechstein Formation. SHC values are mainly between approximately 900 and 2400 J/(kg K) with the lowest values provided by the Zechstein Formation and an increasing trend with shallower depth for the overlying formations. The majority of formation RHP values range from  $< 0.1$  to  $2.5 \mu\text{W}/\text{m}^3$ . The lowest amount of heat generation is observed in the carbonates (Chalk Group; mean:  $0.15 \pm 0.15 \mu\text{W}/\text{m}^3$ ) and evaporites (Zechstein Formation; mean:  $0.13 \pm 0.06 \mu\text{W}/\text{m}^3$ ). Formations dominated by clastic rocks show an RHP of 0.3 to  $2.5 \text{ W}/(\text{m K})$  (mean:  $1.0 \pm 0.02 \mu\text{W}/\text{m}^3$ )

The lateral variability of mean formation values is illustrated in Fig. 6 (lower panel) and is quantified by Eq. (7) and the (1-sigma) standard deviation. The variability of mean formation values (without the Post Chalk section), adjusted for the effect of the methodological

uncertainties (cf. Section 5.1), ranges between 13 and 49% (mean:  $23 \pm 11\%$ ) for TC, between 11 and 65% (mean:  $34 \pm 16\%$ ) for TD, between 0 and 31% (mean:  $16 \pm 8\%$ ) for SHC, and between 5 and  $> 100\%$  (mean:  $64 \pm 24\%$ ) for RHP. The standard deviation of the mean formation values ranges between approximately 0.3 and  $1.1 \text{ W}/(\text{m K})$  for TC (lowest SD for the homogeneous Chalk Group, highest for the heterogeneous Tønder Formation; average SD:  $0.5 \text{ W}/(\text{m K})$ ), between approximately 0.1 and  $0.5 \cdot 10^{-6} \text{ m}^2/\text{s}$  for TD (lowest SD for Flyvbjerg Member, highest for Tønder Formation; average  $0.3 \cdot 10^{-6} \text{ m}^2/\text{s}$ ), between approximately 110 and 280 J/(kg K) for SHC (lowest for Zechstein Formation, highest for Tønder Formation; average  $200 \text{ J}/(\text{kg K})$ ), and between 0.06 and  $0.68 \mu\text{W}/\text{m}^3$  for RHP (lowest for Zechstein Formation, highest for Tønder Formation; average  $0.3 \mu\text{W}/\text{m}^3$ ), respectively.

### 5.3. Effect on modelled geotherms

The effect of the basin-wide TC variation on the subsurface temperature is quantified by conducting 1D temperature models at three well locations. For each well, the modelled geotherms show large variations depending on the local geology and the implemented formation

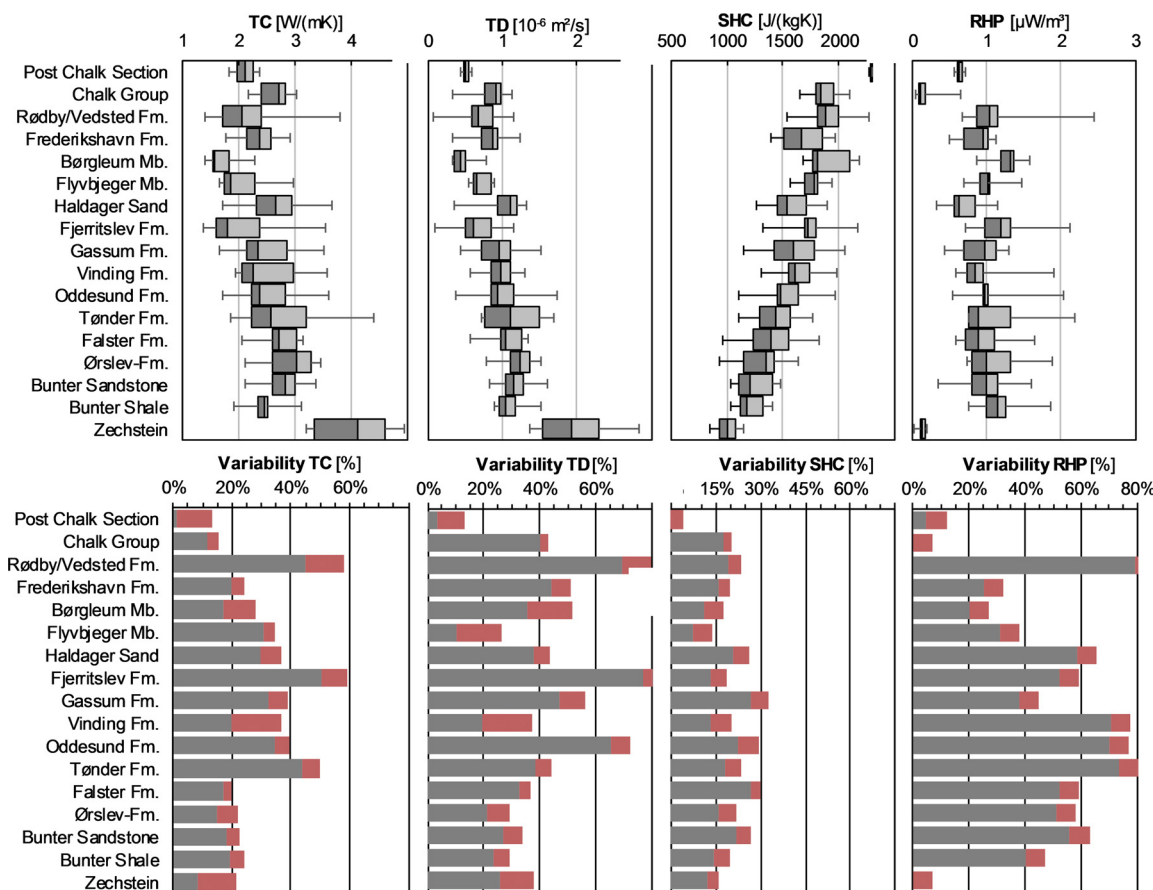


**Fig. 6.** Upper panels: boxplot (min,  $Q_{0.25}$ , median,  $Q_{0.75}$ , max) of the mean formation values of thermal conductivity (TC), thermal diffusivity (TD), specific heat capacity (SHC), and radiogenic heat production (RHP). Lower panels: Maximum variability (dark grey bars) and average prediction uncertainties (red-cross-hatched fraction of the maximum variability) of mean formation values (For interpretation of the references to color in this figure legend, the reader is referred to the web version of this article).

TC values. The results are visualized in Fig. 7, where the implemented heat-flow profiles are shown as well, and summarized in Table 2.

For the Aars-1/1 A well (Fig. 7; A), the predicted temperature at a depth of approximately 3200 m ranges between a minimum of 69 °C (maximum basin formation TC values) and a maximum of 122 °C (minimum basin formation TC), and the delta is 53 °C. The temperature at that depth predicted from the average basin formation conductivity is 86 °C, whereas the temperature logged during the 2014 campaign recorded values of 107 °C (pers. communication N. Balling). Computations with a continuous TC profile results in a temperature of 102 °C at that depth. The additional consideration of a well-specific heat-flow profile yields 107 °C and thus the closest fit to the measured temperatures. The averaged absolute misfit to the logged temperatures along the borehole is  $19.0 \pm 4.3\%$  for the application of mean formation TC values and regional heat flow,  $8.6 \pm 2.7\%$  for a continuous TC profile and regional heat flow, and  $1.5 \pm 0.6\%$  for a continuous TC profile and a site-specific heat-flow profile.

For the Stenlille-1 well (Fig. 7; B), the predicted temperature at a depth of approximately 1250 m is in the range of 30–41 °C (delta: 11 °C). The predicted temperature from the average basin formation conductivity is 33 °C, whereas the logged temperature (1986 campaign) is 41 °C. The application of continuous TC profiles computes 36 °C (with regional heat flow) and 41 °C (with a site-specific heat-flow profile). The averaged absolute misfits are  $13.9 \pm 3.5\%$ ,  $4.2 \pm 3.5\%$ , and  $1.8 \pm 0.7\%$ , respectively.

For the deepest well, Mors-1 (Fig. 7; C), the predicted temperature at a depth of 5200 m is in the range of 120–225 °C (delta: 105 °C). The predicted temperature from the application of mean basin formation

conductivity is 157 °C, whereas the corrected bottom-hole temperature is reported as 135 °C (Poulsen et al., 2012). The application of a continuous TC profile and regional heat flow results in 127 °C the maximum depth and thus a misfit of approximately 8 °C (6%).

## 6. Discussion

### 6.1. Reliability of the computed mean formation thermal properties in the Danish Basin

Profiles of petrophysical properties ( $\lambda$ ,  $\alpha$ ,  $c_p$ ,  $H$ ,  $\varphi$ , and  $\rho_b$ ) were calculated from geophysical logs at 23 wells in the DB. Rock thermal property profiles were predicted from combinations of VSH, RHOB, DT, U and PHIN with at least three geophysical well logs to minimize the expected absolute prediction error along the borehole (usually 5–10% for 3–5 logs). The predicted profile with the smallest uncertainty (according to the Appendices of Fuchs et al., 2015) is used as the best prediction profile. All the predicted profiles of a specific parameter were used to quantify the uncertainty of the mean formation values resulting from the use of varying well-log combinations. For all the wells, these additional uncertainties averaged 11% (TC), 14% (TD), and 7% (SHC) (Section 6.1) and need to be considered when the regional variability of mean formation values is analysed.

A validation of the predicted profiles on measured core data is desirable, but could not be realized systematically because of a lack of sufficiently dense sampled data on rock thermal properties in the DB as well as the general challenges for this term discussed in the background chapter. In particular, data for TD and SHC are not available. For TC

**Table 1**  
Variability of mean formation values for petrophysical rock properties in the Danish Basin.

| System                 | Formation            | Thermal conductivity [W/(m K)]   |      |      |                   |                  |                   |      |    | Thermal diffusivity [ $10^{-6}$ m <sup>2</sup> /s]    |      |      |                   |                  |                   |      |    |
|------------------------|----------------------|----------------------------------|------|------|-------------------|------------------|-------------------|------|----|---|------|------|-------------------|------------------|-------------------|------|----|
|                        |                      | mean                             | sd   | min  | Q <sub>0.25</sub> | Q <sub>0.5</sub> | Q <sub>0.75</sub> | max  | n  | mean  | sd   | min  | Q <sub>0.25</sub> | Q <sub>0.5</sub> | Q <sub>0.75</sub> | max  | n  |
| Cenozoic<br>Cretaceous | Post Chalk Section   | 2.11                             | 0.39 | 1.83 | 1.97              | 2.11             | 2.24              | 2.38 | 2  | 0.51  | 0.10 | 0.45 | 0.48              | 0.51             | 0.55              | 0.58 | 2  |
|                        | Chalk Group          | 2.64                             | 0.26 | 2.19 | 2.39              | 2.72             | 2.83              | 3.02 | 21 | 0.85  | 0.21 | 0.33 | 0.76              | 0.92             | 0.97              | 1.12 | 21 |
|                        | Rødby/Vedsted Fm.    | 2.09                             | 0.70 | 1.41 | 1.73              | 2.06             | 2.41              | 3.80 | 22 | 0.69  | 0.23 | 0.08 | 0.59              | 0.67             | 0.87              | 1.15 | 22 |
| Jurassic               | Frederikshavn Fm.    | 2.35                             | 0.34 | 1.77 | 2.13              | 2.37             | 2.58              | 2.92 | 17 | 0.83  | 0.20 | 0.34 | 0.71              | 0.88             | 0.94              | 1.24 | 17 |
|                        | Børgleum Mb.         | 1.71                             | 0.29 | 1.42 | 1.53              | 1.57             | 1.84              | 2.29 | 10 | 0.48  | 0.15 | 0.33 | 0.36              | 0.44             | 0.51              | 0.79 | 10 |
|                        | Flyvbjerg Mb.        | 2.08                             | 0.46 | 1.67 | 1.75              | 1.87             | 2.29              | 2.96 | 7  | 0.72  | 0.14 | 0.56 | 0.61              | 0.65             | 0.85              | 0.90 | 7  |
| Triassic               | Haldager Sand        | 2.66                             | 0.51 | 1.71 | 2.31              | 2.66             | 2.94              | 3.65 | 15 | 1.01  | 0.26 | 0.35 | 0.93              | 1.12             | 1.19              | 1.32 | 15 |
|                        | Fjerritslev Fm.      | 1.98                             | 0.68 | 1.38 | 1.60              | 1.81             | 2.36              | 3.54 | 20 | 0.67  | 0.27 | 0.29 | 0.51              | 0.62             | 0.85              | 1.15 | 20 |
|                        | Gassum Fm.           | 2.50                             | 0.55 | 1.67 | 2.13              | 2.35             | 2.86              | 3.51 | 21 | 0.97  | 0.28 | 0.45 | 0.72              | 0.96             | 1.11              | 1.53 | 21 |
|                        | Vinding Fm.          | 2.54                             | 0.60 | 1.93 | 2.04              | 2.24             | 2.98              | 3.58 | 19 | 0.98  | 0.22 | 0.58 | 0.86              | 0.97             | 1.11              | 1.30 | 19 |
|                        | Oddesund Fm.         | 2.53                             | 0.60 | 1.71 | 2.24              | 2.38             | 2.83              | 3.60 | 12 | 0.99  | 0.39 | 0.37 | 0.85              | 0.94             | 1.15              | 1.73 | 12 |
|                        | Tønder Fm.           | 2.85                             | 1.11 | 1.85 | 2.22              | 2.57             | 3.20              | 4.41 | 6  | 1.15  | 0.48 | 0.72 | 0.76              | 1.10             | 1.49              | 1.69 | 6  |
|                        | Falster Fm.          | 2.74                             | 0.34 | 2.07 | 2.61              | 2.71             | 3.02              | 3.15 | 12 | 1.08  | 0.23 | 0.58 | 0.99              | 1.05             | 1.26              | 1.35 | 12 |
|                        | Ørslev-Fm.           | 2.93                             | 0.43 | 2.11 | 2.60              | 3.03             | 3.29              | 3.45 | 10 | 1.22  | 0.22 | 0.79 | 1.10              | 1.23             | 1.37              | 1.52 | 10 |
|                        | Bunter Sandstone     | 2.80                             | 0.35 | 2.11 | 2.60              | 2.82             | 2.99              | 3.37 | 12 | 1.18  | 0.23 | 0.83 | 1.05              | 1.16             | 1.27              | 1.61 | 12 |
|                        | Bunter Shale         | 2.51                             | 0.38 | 1.93 | 2.35              | 2.47             | 2.50              | 3.12 | 11 | 1.09  | 0.18 | 0.90 | 0.97              | 1.06             | 1.17              | 1.51 | 11 |
| Permian                | Zechstein            | 4.09                             | 0.83 | 3.20 | 3.34              | 4.11             | 4.60              | 4.95 | 7  | 1.97  | 0.48 | 1.37 | 1.54              | 1.93             | 2.29              | 2.84 | 7  |
|                        | min <sup>a</sup>     | 1.71                             | 0.26 | 1.38 | 1.53              | 1.57             | 1.84              | 2.29 |    | 0.48  | 0.14 | 0.08 | 0.36              | 0.44             | 0.51              | 0.58 |    |
|                        | average <sup>a</sup> | 2.53                             | 0.53 | 1.88 | 2.21              | 2.46             | 2.81              | 3.39 |    | 0.96  | 0.26 | 0.55 | 0.81              | 0.95             | 1.11              | 1.37 |    |
|                        | max <sup>a</sup>     | 4.09                             | 1.11 | 3.20 | 3.34              | 4.11             | 4.60              | 4.95 |    | 1.97  | 0.48 | 1.37 | 1.54              | 1.93             | 2.29              | 2.84 |    |
| System                 | Formation            | Specific heat capacity [J/(kgK)] |      |      |                   |                  |                   |      |    | Radiogenic heat production [ $\mu$ W/m <sup>3</sup> ] |      |      |                   |                  |                   |      |    |
|                        |                      | mean                             | sd   | min  | Q <sub>0.25</sub> | Q <sub>0.5</sub> | Q <sub>0.75</sub> | max  | n  | mean  | sd   | min  | Q <sub>0.25</sub> | Q <sub>0.5</sub> | Q <sub>0.75</sub> | max  | n  |
| Cenozoic<br>Cretaceous | Post Chalk Section   | 2283                             | 19   | 2269 | 2276              | 2283             | 2289              | 2296 | 2  | 0.64  | 0.11 | 0.56 | 0.60              | 0.64             | 0.67              | 0.71 | 2  |
|                        | Chalk Group          | 1894                             | 180  | 1653 | 1798              | 1840             | 1950              | 2402 | 21 | 0.15  | 0.14 | 0.04 | 0.08              | 0.12             | 0.17              | 0.64 | 18 |
|                        | Rødby/Vedsted Fm.    | 1907                             | 197  | 1529 | 1802              | 1877             | 1994              | 2412 | 22 | 1.06  | 0.35 | 0.67 | 0.86              | 1.03             | 1.14              | 2.45 | 23 |
| Jurassic               | Frederikshavn Fm.    | 1681                             | 203  | 1395 | 1514              | 1665             | 1851              | 2050 | 17 | 0.87  | 0.21 | 0.50 | 0.70              | 0.96             | 1.01              | 1.12 | 16 |
|                        | Børgleum Mb.         | 1912                             | 219  | 1677 | 1772              | 1811             | 2093              | 2307 | 10 | 1.25  | 0.22 | 0.86 | 1.18              | 1.31             | 1.36              | 1.58 | 10 |
|                        | Flyvbjerg Mb.        | 1774                             | 155  | 1567 | 1692              | 1780             | 1815              | 2057 | 7  | 1.01  | 0.24 | 0.70 | 0.90              | 1.02             | 1.02              | 1.47 | 7  |
| Triassic               | Haldager Sand        | 1601                             | 231  | 1271 | 1452              | 1531             | 1707              | 2071 | 15 | 0.69  | 0.22 | 0.32 | 0.55              | 0.63             | 0.83              | 1.15 | 15 |
|                        | Fjerritslev Fm.      | 1726                             | 135  | 1320 | 1688              | 1727             | 1797              | 1956 | 20 | 1.22  | 0.38 | 0.71 | 0.98              | 1.19             | 1.32              | 2.12 | 23 |
|                        | Gassum Fm.           | 1608                             | 275  | 1143 | 1416              | 1587             | 1776              | 2182 | 21 | 0.92  | 0.25 | 0.43 | 0.68              | 0.97             | 1.12              | 1.30 | 23 |
|                        | Vinding Fm.          | 1636                             | 176  | 1305 | 1548              | 1604             | 1742              | 1961 | 19 | 0.91  | 0.35 | 0.59 | 0.73              | 0.84             | 0.95              | 1.90 | 11 |
|                        | Oddesund Fm.         | 1529                             | 251  | 1106 | 1445              | 1482             | 1631              | 1972 | 12 | 1.07  | 0.43 | 0.54 | 0.94              | 0.97             | 1.02              | 2.03 | 8  |
|                        | Tønder Fm.           | 1433                             | 279  | 1103 | 1291              | 1430             | 1572              | 1770 | 6  | 1.18  | 0.68 | 0.75 | 0.75              | 0.89             | 1.32              | 2.19 | 4  |
|                        | Falster Fm.          | 1391                             | 238  | 965  | 1237              | 1390             | 1552              | 1791 | 12 | 0.98  | 0.38 | 0.59 | 0.70              | 0.89             | 1.11              | 1.65 | 10 |
|                        | Ørslev-Fm.           | 1273                             | 213  | 931  | 1147              | 1356             | 1418              | 1530 | 10 | 1.07  | 0.38 | 0.72 | 0.80              | 0.99             | 1.31              | 1.87 | 10 |
|                        | Bunter Sandstone     | 1277                             | 220  | 1039 | 1107              | 1204             | 1413              | 1680 | 12 | 0.98  | 0.37 | 0.35 | 0.80              | 1.00             | 1.16              | 1.61 | 10 |
|                        | Bunter Shale         | 1230                             | 159  | 1028 | 1117              | 1173             | 1321              | 1485 | 11 | 1.17  | 0.34 | 0.77 | 0.99              | 1.15             | 1.26              | 1.85 | 9  |
| Permian                | Zechstein            | 1007                             | 114  | 850  | 933               | 1007             | 1072              | 1173 | 7  | 0.13  | 0.06 | 0.02 | 0.10              | 0.14             | 0.16              | 0.20 | 8  |
|                        | min <sup>a</sup>     | 1007                             | 114  | 850  | 933               | 1007             | 1072              | 1173 |    | 0.13  | 0.06 | 0.02 | 0.08              | 0.12             | 0.16              | 0.20 |    |
|                        | average <sup>a</sup> | 1598                             | 203  | 1303 | 1484              | 1573             | 1706              | 1947 |    | 0.90  | 0.31 | 0.54 | 0.73              | 0.87             | 1.00              | 1.52 |    |
|                        | max <sup>a</sup>     | 2283                             | 279  | 2269 | 2276              | 2283             | 2289              | 2412 |    | 1.25  | 0.68 | 0.86 | 1.18              | 1.31             | 1.36              | 2.45 |    |
| System                 | Formation            | Porosity [n/n]                   |      |      |                   |                  |                   |      |    | Bulk density [g/cm <sup>3</sup> ]                     |      |      |                   |                  |                   |      |    |
|                        |                      | mean                             | sd   | min  | Q <sub>0.25</sub> | Q <sub>0.5</sub> | Q <sub>0.75</sub> | max  | n  | mean  | sd   | min  | Q <sub>0.25</sub> | Q <sub>0.5</sub> | Q <sub>0.75</sub> | max  | n  |
| Cenozoic<br>Cretaceous | Post Chalk Section   | n.a.                             | n.a. | n.a. | n.a.              | n.a.             | n.a.              | n.a. | 0  | n.a.  | n.a. | n.a. | n.a.              | n.a.             | n.a.              | n.a. | 0  |
|                        | Chalk Group          | 0.25                             | 0.04 | 0.19 | 0.23              | 0.24             | 0.27              | 0.32 | 17 | 2.44  | 0.08 | 2.25 | 2.41              | 2.46             | 2.49              | 2.52 | 15 |
|                        | Rødby/Vedsted Fm.    | 0.32                             | 0.05 | 0.16 | 0.29              | 0.32             | 0.34              | 0.40 | 21 | 2.26  | 0.08 | 2.08 | 2.21              | 2.27             | 2.30              | 2.38 | 21 |
| Jurassic               | Frederikshavn Fm.    | 0.26                             | 0.04 | 0.19 | 0.23              | 0.27             | 0.29              | 0.33 | 15 | 2.32  | 0.08 | 2.16 | 2.27              | 2.35             | 2.37              | 2.43 | 15 |
|                        | Børgleum Mb.         | 0.31                             | 0.04 | 0.26 | 0.29              | 0.30             | 0.32              | 0.38 | 10 | 2.32  | 0.09 | 2.20 | 2.28              | 2.29             | 2.40              | 2.47 | 9  |
|                        | Flyvbjerg Mb.        | 0.27                             | 0.03 | 0.25 | 0.25              | 0.26             | 0.28              | 0.34 | 7  | 2.29  | 0.06 | 2.19 | 2.27              | 2.28             | 2.32              | 2.39 | 7  |
| Triassic               | Haldager Sand        | 0.23                             | 0.06 | 0.15 | 0.20              | 0.22             | 0.29              | 0.33 | 13 | 2.32  | 0.10 | 2.19 | 2.25              | 2.30             | 2.38              | 2.56 | 14 |
|                        | Fjerritslev Fm.      | 0.29                             | 0.04 | 0.17 | 0.26              | 0.28             | 0.31              | 0.38 | 21 | 2.36  | 0.09 | 2.15 | 2.30              | 2.37             | 2.42              | 2.52 | 20 |
|                        | Gassum Fm.           | 0.25                             | 0.07 | 0.10 | 0.22              | 0.26             | 0.29              | 0.39 | 22 | 2.33  | 0.08 | 2.19 | 2.26              | 2.33             | 2.38              | 2.46 | 21 |
|                        | Vinding Fm.          | 0.26                             | 0.05 | 0.16 | 0.22              | 0.28             | 0.29              | 0.33 | 10 | 2.34  | 0.08 | 2.23 | 2.29              | 2.32             | 2.39              | 2.48 | 10 |
|                        | Oddesund Fm.         | 0.23                             | 0.06 | 0.12 | 0.21              | 0.24             | 0.28              | 0.30 | 8  | 2.37  | 0.07 | 2.29 | 2.32              | 2.34             | 2.40              | 2.48 | 7  |
|                        | Tønder Fm.           | 0.25                             | 0.09 | 0.12 | 0.23              | 0.28             | 0.29              | 0.30 | 4  | 2.36  | 0.05 | 2.29 | 2.34              | 2.37             | 2.40              | 2.41 | 4  |
|                        | Falster Fm.          | 0.18                             | 0.06 | 0.09 | 0.15              | 0.20             | 0.21              | 0.27 | 9  | 2.51  | 0.06 | 2.39 | 2.51              | 2.53             | 2.56              | 2.58 | 9  |
|                        | Ørslev-Fm.           | 0.17                             | 0.06 | 0.06 | 0.19              | 0.19             | 0.21              | 0.22 | 9  | 2.50  | 0.09 | 2.35 | 2.45              | 2.49             | 2.57              | 2.62 | 9  |
|                        | Bunter Sandstone     | 0.18                             | 0.06 | 0.09 | 0.13              | 0.20             | 0.22              | 0.25 | 8  | 2.46  | 0.07 | 2.36 | 2.39              | 2.46             | 2.50              | 2.57 | 9  |
|                        | Bunter Shale         | 0.17                             | 0.06 | 0.03 | 0.15              | 0.18             | 0.20              | 0.23 | 8  | 2.51  | 0.08 | 2.38 | 2.48              | 2.51             | 2.56              | 2.64 | 8  |
| Permian                | Zechstein            | 0.06                             | 0.05 | 0.01 | 0.02              | 0.05             | 0.10              | 0.14 | 7  | 2.48  | 0.19 | 2.25 | 2.34              | 2.48             | 2.67              | 2.72 | 9  |
|                        | min <sup>a</sup>     | 0.06                             | 0.03 | 0.01 | 0.02              | 0.05             | 0.10              | 0.14 |    | 2.26  | 0.05 | 2.08 | 2.21              | 2.27             | 2.30              | 2.38 |    |
|                        | average <sup>a</sup> | 0.23                             | 0.05 | 0.13 | 0.21              | 0.24             | 0.26              | 0.31 |    | 2.39  | 0.08 | 2.25 | 2.34              | 2.39             | 2.44              | 2.52 |    |
|                        | max <sup>a</sup>     | 0.32                             | 0.09 | 0.26 | 0.29              | 0.32             | 0.34              | 0.40 |    | 2.51  | 0.19 | 2.39 | 2.51              | 2.53             | 2.67              | 2.72 |    |

Note: <sup>a</sup> The Post Chalk section is excluded from the computation min/average/max of the standard deviation, according to the small number of samples.

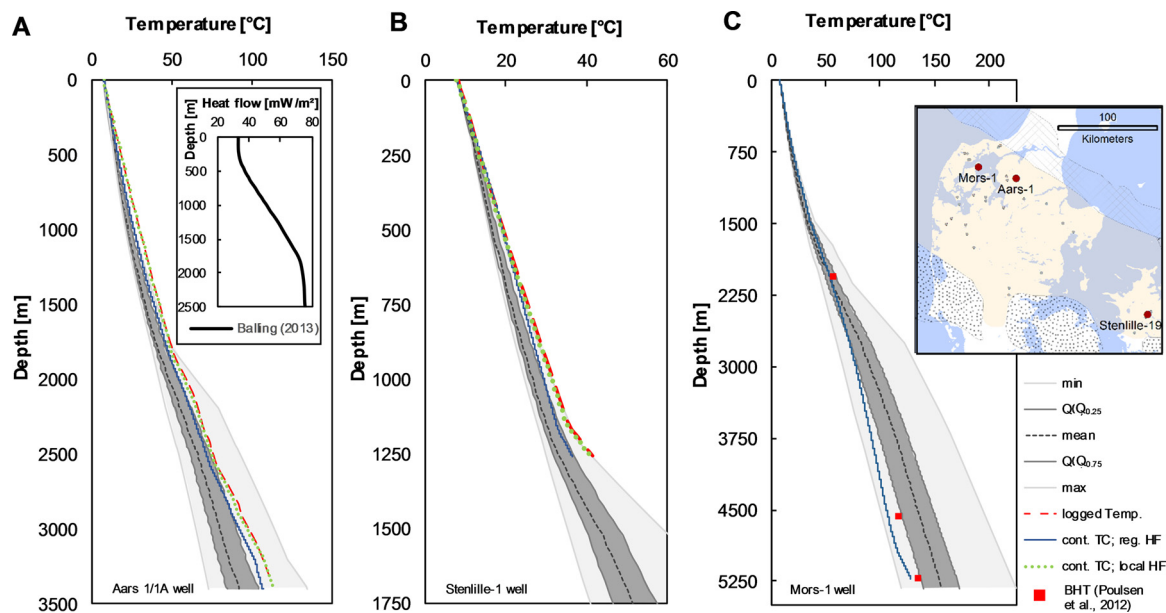


Fig. 7. 1D temperature profiles calculated from formation TC values for three wells in the DB. Plots show logged temperature profiles (red dashed line), measured BHT values (red filled squares), the envelope of the predicted temperature profiles (light grey: maximum range; dark grey: inner 50%); predicted temperature from continuous TC profiles based on the regional heat-flow profile of Balling, 2013 (blue solid line) and the site-specific heat flow (Balling et al., in preparation). The general HF profile is shown in panel A. The results are summarized for maximum depth in Table 1. Note: varying depth scales (For interpretation of the references to color in this figure legend, the reader is referred to the web version of this article).

and to some extent RHP, the most comprehensive studies are provided by Balling (1979) and Balling et al. (1981) and allow at least a credible comparison for the lithologically very homogeneous Chalk Group. Balling and co-workers measured TC values in the range of approximately 1.6–2.8 W/(m K) that average  $2.3 \pm 0.3$  W/(m K). In the present study mean formation values in the range of 2.2–3.0 W/(m K), that average  $2.6 \pm 0.3$  W/(m K), are slightly higher, but in good agreement with the previously published results.

It also needs to be considered that considerable anisotropies were observed in the past for some rocks of the selected stratigraphy in the DB (cf. Balling et al., 1992). However, the anisotropy of TC and TD cannot be extracted from the well logs with the selected approach.

## 6.2. Mean formation values and their regional variability

### 6.2.1. Thermal conductivity

The formation TC values of 1.7–4.4 W/(m K) determined for Late Permian to Cenozoic formations are in the range of common values expected for sedimentary rocks (cf. Schön, 2011). As this is the first study of its kind for this field, no equivalent TC data are published that could be used in a detailed comparison of the same grade. However, some indications can be taken from recent petrophysical studies in the North German Basin (NGB). The (Mesozoic) mean formation TC inverted from temperature-log values are published in the range of 1.5–3.1 W/(m K) (one well; Fuchs and Förster, 2010), 1.5–3.9 W/(m K) (15 wells; Schütz et al., 2013), 1.8–3.5 W/(m K), (one well; Sippel et al.,

Table 2  
Variation in modelled temperature at depth with maximum recorded temperature.

| Well        | Depth [m] | Measured Temp. [°C] | Based on formation mean TC values and regional HF |                        |           |                        |          |                 |                        |           |                      |           |                 |           |          |
|-------------|-----------|---------------------|---|------------------------|-----------|------------------------|----------|-----------------|------------------------|-----------|----------------------|-----------|-----------------|-----------|----------|
|             |           |                     | Predicted   |                        |           |                        |          |                 | Missfit of mean progn. |           | Missfit of inner 50% |           | Maximum missfit |           |          |
|             |           |                     | min [°C]  | Q <sub>0.25</sub> [°C] | mean [°C] | Q <sub>0.75</sub> [°C] | max [°C] | Full range [°C] | 50% range [°C]         | abs. [°C] | rel. [%]             | abs. [°C] | rel. [%]        | abs. [°C] | rel. [%] |
| Aars-1      | 3200      | 107.2               | 69.4  | 79.2                   | 85.6      | 96.7                   | 122.3    | 53.0            | 17.5                   | -21.5     | -20%                 | 10.5–28   | -10% to -26%    | -37.8     | -35%     |
| Stenlille-1 | 1250      | 41.0                | 29.9  | 31.7                   | 33.0      | 36.6                   | 40.7     | 10.9            | 4.9                    | -8.0      | -20%                 | 4.5–9.3   | -11% to -23%    | -11.1     | -27%     |
| Moors-1     | 5214      | 135.0               | 119.4   | 139.9                  | 156.8     | 173.1                  | 224.7    | 105.3           | 33.2                   | 21.8      | 16%                  | 5–38      | 4%–28%          | 89.7      | 66%      |

| Well        | Depth [m] | Measured Temp. [°C] | Based on cont. TC profiles and regional HF |      |           | Based on cont. TC profiles and local HF |      |           |
|-------------|-----------|---------------------|--|------|-----------|---|------|-----------|
|             |           |                     | Predicted                                  |      | Missfit   | Predicted                               |      | Missfit   |
|             |           |                     | [°C]                                       | [°C] | abs. [°C] | rel. [%]                                | [°C] | abs. [°C] |
| Aars-1      | 3200      | 107.2               | 101.7                                      | -5.4 | -5%       | 107.7                                   | 0.5  | < 1%      |
| Stenlille-1 | 1250      | 41.0                | 36.2                                       | -4.9 | -12%      | 40.7                                    | -0.4 | < 1%      |
| Moors-1     | 5214      | 135.0               | n.a.                                       | n.a. | n.a.      | n.a.                                    | n.a. | n.a.      |

2013), 1.9–3.1 W/(m K) (25 wells; Fuchs and Balling, 2016b). The overall range of mean formation values for TC are quite comparable to the present study for the DB. Based on the data of Schütz et al. (2013), and Fuchs and Balling (2016b) the variability of mean formation TC can also be calculated. The variability ranges between 15 and 39% (mean:  $22 \pm 10\%$ ) for data reported by Schütz et al. (2013) are remarkably close to the variability identified by the approach presented in this paper (range: 13–49%, mean:  $23 \pm 11\%$ ). The variability computed from the data of Fuchs and Balling (2016b) is between 11 and 49% (mean:  $36 \pm 11\%$ ). Data from this study shows larger variability but are uncorrected in terms of the uncertainties introduced by the use of varying well-log combinations (cf. Section 6.1). Considering average uncertainty identified reduces the mean variability to approximately 25% and the maximum variability to approximately 38%, which is close to the observations of the present study as well.

### 6.2.2. Radiogenic heat production

The Mesozoic mean formation RHP values of up to  $2.5 \mu\text{W}/\text{m}^3$  (minimum of  $0.3 \mu\text{W}/\text{m}^3$  for clastic-dominated formations; mean:  $0.9 \pm 0.3 \mu\text{W}/\text{m}^3$ ) determined from the DB samples are almost identical to the values between 0 and  $2.5 \mu\text{W}/\text{m}^3$  (mean:  $1.1 \pm 0.7 \mu\text{W}/\text{m}^3$ ) measured by Balling et al. (1981) from drill core samples in the DB and in a line with log-derived values of  $0.4\text{--}1.8 \mu\text{W}/\text{m}^3$  reported by Norden and Förster (2006) for post-Permian sediments in the NGB. Claystone-rich formations, like the Børglum Member or the Fjerritslev Formation show the highest heat production in the DB (means:  $1.25 \pm 0.22 \mu\text{W}/\text{m}^3$  and  $1.22 \pm 0.38 \mu\text{W}/\text{m}^3$ ), whereas limestones and evaporite rocks of the Chalk Group and the Permian Zechstein Formation consistently show the lowest heat production, usually between 0 and  $0.3 \mu\text{W}/\text{m}^3$  (means:  $0.15 \pm 0.14 \mu\text{W}/\text{m}^3$  and  $0.13 \pm 0.06 \mu\text{W}/\text{m}^3$ , respectively). With the exception of the latter two, the majority of geological formations show a maximum variability in the RHP (typical range: 30–80%) much larger than that for TC, in agreement with previous observations from core studies (e.g., Vilà et al., 2010).

### 6.2.3. Specific heat capacity and thermal diffusivity

Mean formation values for SHC range between 900 and  $2500 \text{ J}/(\text{kg K})$  and are thereby in the common range expected for sedimentary rocks (Schön, 2011). As water has a SHC five to seven times higher than that of the mineral rock matrix (usually between 550 and  $850 \text{ J}/(\text{kg K})$ ), porosity and the pore-filling fluid water dominate the bulk SHC. As porosity is to some extent also a function of depth, a general trend of decreasing porosity with depth is consequently obtained from our analysis. The highest values for bulk SHC of  $> 1900 \text{ J}/(\text{kg K})$  are observed only for the shallow formations of Cenozoic and Cretaceous age. Jurassic and Triassic units, in contrast, range between 1200 and  $1900 \text{ J}/(\text{kg K})$  and deep Zechstein evaporites average a minimum of approximately  $1000 \text{ J}/(\text{kg K})$ . This observation is also supported by the non-correlation of SHC with the formation sandstone or shale fraction. The maximum variability of formation SHC ranges between 0 and 31% and averages approximately  $16 \pm 8\%$ . It is significantly lower than the variability of formation values observed for TC and RHP. Formation values for SHC and TD were not determined in previous studies and hence could not be used for comparison.

### 6.3. Effect on temperature models

The forward computation of 1D-borehole geotherms reveals the large impact of the variability of formation TC on the subsurface temperature. Considering the basin-wide mean formation conductivity (cf. Table 2), the misfit between predicted temperature (at maximum depth) and measured temperature is on the order of 20% (range:  $-21 \text{ }^\circ\text{C}$ – $21.8 \text{ }^\circ\text{C}$ ) for all three wells. The largest temperature deviations are on the order of 27–66% (range:  $-38$  to  $90 \text{ }^\circ\text{C}$ ). Both results demonstrate the strong impact of regional rock TC variability on the predicted subsurface temperatures. The often-taken assumption that

observations of rock/formation TC from single locations in a basin are a sufficiently representative parameter for geothermal models is not supported by our data and afflicted with large uncertainties in modelled temperatures. For the present analysis, uncertainties of the modelled temperatures are introduced on the order of  $\pm 20\%$  on average by using basin wide homogenous rock TC values for geological formations. In the case of a poor or even unlucky selection (extreme value in terms of the basin mean) of the particular anchor well, this effect can locally be identified and easily multiplied (to factor 2 or 3). For the case that numerical temperature models (with constant layer parameter values) are calibrated against observations, the present study gives some indication as to the amount of uncertainty that has to be taken into account in areas where no temperature control is available. Steps towards improving the reliability of subsurface temperature models, including models for the DB and the northern part of the NGB, were taken by Fuchs and Balling (2016a); Balling et al. (2016) and Poulsen et al. (2017) by applying inverse model calibration procedures, where initial estimates of model layer conductivities were adjusted to obtain the best agreement with measured borehole temperatures, where available. Further improvements may be obtained by using the present procedure with log-derived TC values as prior estimates for inverse parameter optimization.

## 7. Summary and conclusion

From this study, a comprehensive set of data on thermal conductivity, thermal diffusivity, specific heat capacity, radiogenic heat production, density, and porosity is now available for future geothermal or hydrocarbon studies in the Danish Basin. The variability of these parameters was systematically studied based on a detailed analysis of geological bore logs and geophysical well-log data from 23 wells in the Danish Basin. In terms of thermal diffusivity and specific heat capacity, the initial application of well logs allowed the initial computation of mean formation values and their variability in the Danish Basin and beyond. The analysis reveals that all the studied formation rock thermal properties display a larger variability than previously applied in geothermal or basin modelling studies. The main conclusions from the presented work can be summarized as follows:

- Using petrophysical well logs for the indirect determination of rock thermal properties can help map their spatial variability and thus significantly reduce uncertainties in modelled temperatures. The present study provides parameter predictions for the Late Permian to Cenozoic depth section but with particular bearing for those sections that are usually out of the focus of hydrocarbon or geothermal exploration campaigns and where few or no data are available.
- In addition to the slightly more common application for thermal conductivity and radiogenic heat production, the present study is the first to demonstrate its novel use for the determination of thermal diffusivity and specific heat capacity.
- The statistical values for geological formations based on continuous log data and are not afflicted with the upscaling problem often seen and discussed in laboratory studies of drill cores or cuttings. The new comprehensive dataset of petrophysical ( $\varphi$  and  $\rho_b$ ) and, in particular, rock thermal properties ( $\lambda$ ,  $\alpha$ ,  $c_p$ , and  $H$ ) for Late Permian to Cenozoic geological formations are therefore available as reliable and unique input for future geothermal models of the Danish Basin.
- Ignoring formation parameter variability happens at the cost of additional and significant uncertainties of modelled results compared to measured temperatures. As our results demonstrate, uncertainties are up to 20% on average and can be even higher locally. These observations can thereby provide helpful advice for reasonable parameter variation limits in the input or post-processing calibration procedure for geothermal models in sedimentary basins of similar genesis to the Danish Basin. The author anticipates that the

well-log-based analysis of the regional thermal-rock-property variability that feeds *a priori* the model parameterisation and *posteriori* the inverse calibration will lead to significantly lower uncertainty in temperature calculations, in particular but not exclusively for areas and depths where temperature observations are unavailable.

## Acknowledgements

This work was performed for the geothermal energy project, funded

## Appendix A

See [Table A1](#).

**Table A1**

Wells in the Danish Basin.

| #  | Well name       | Year | Status   | Latitude     | Longitude    | Depth [m] |
|----|-----------------|------|----------|--------------|--------------|-----------|
| 1  | Aars-1/1 A      | 1979 | studied  | 56°47'43.53" | 09°30'33.76" | 1,685     |
| 2  | Farsø-1         | 1982 | studied  | 56°46'53.04" | 09°21'49.68" | 2,928     |
| 3  | Felicia-1       | 1987 | studied  | 57°26'17.60" | 08°18'41.02" | 5,281     |
| 4  | Hobro-1         | 1974 | studied  | 56°36'30.00" | 09°38'04.00" | 2,578     |
| 5  | Hyllebjerg-1    | 1976 | studied  | 56°48'53.00" | 09°20'54.00" | 2,855     |
| 6  | Jelling-1       | 1992 | studied  | 55°44'21.50" | 09°22'33.00" | 1,933     |
| 7  | Karlebo-1/1 A   | 2007 | studied  | 55°55'12.90" | 12°25'04.09" | 2,444     |
| 8  | Kvols-1         | 1976 | studied  | 56°31'49.00" | 09°17'56.00" | 2,622     |
| 9  | Linde-1         | 1980 | studied  | 56°26'00.05" | 08°26'30.25" | 2,213     |
| 10 | Løve-1          | 2011 | studied  | 55°48'08.02" | 09°22'52.47" | 2,375     |
| 11 | Mejrup-1        | 1987 | studied  | 56°22'38.90" | 08°40'36.30" | 2,482     |
| 12 | Mors-1          | 1967 | studied  | 56°54'00.00" | 08°53'05.00" | 5,303     |
| 13 | Nøvling-1       | 1966 | studied  | 56°10'09.00" | 08°48'36.00" | 3,700     |
| 14 | Oddesund-1      | 1976 | studied  | 56°33'36.70" | 08°34'10.10" | 3,540     |
| 15 | Rødding-1       | 1976 | studied  | 56°38'49.00" | 08°48'18.00" | 2,163     |
| 16 | Rønde-1         | 1966 | studied  | 56°18'14.00" | 10°26'06.00" | 5,259     |
| 17 | Skive-1         | 1976 | studied  | 56°37'38.00" | 09°00'11.00" | 2,290     |
| 18 | Skive-2         | 1985 | studied  | 56°35'37.70" | 09°00'21.20" | 1,421     |
| 19 | Stenlille-1     | 1980 | studied  | 55°32'38.24" | 11°37'06.41" | 1,622     |
| 20 | Stenlille-19    | 2000 | studied  | 55°32'01.03" | 11°35'55.30" | 2,521     |
| 21 | Thisted-2       | 1982 | studied  | 56°57'55.97" | 08°42'56.73" | 3,251     |
| 22 | Thisted-4       | 1985 | studied  | 57°01'16.81" | 08°41'53.18" | 3,381     |
| 23 | Voldum-1        | 1974 | studied  | 56°23'02.20" | 10°16'00.70" | 2,277     |
| 24 | C-1X            | 1968 | screened | 56°36'41.50" | 07°40'00.00" | 3,208     |
| 25 | Erslev-1        | 1980 | screened | 56°48'09.80" | 08°46'14.90" | 3,465     |
| 26 | Erslev-2        | 1980 | screened | 56°48'43.26" | 08°46'31.12" | 3,397     |
| 27 | Fjerritslev-1   | 1958 | screened | 57°04'52.00" | 09°12'56.00" | 910       |
| 28 | Fjerritslev-2   | 1958 | screened | 57°05'46.00" | 09°15'05.00" | 2,337     |
| 29 | Gassum-1        | 1951 | screened | 56°33'45.00" | 10°00'18.00" | 3,404     |
| 30 | Horsens-1       | 1958 | screened | 55°56'11.10" | 09°54'13.24" | 1,672     |
| 31 | Lavø-1          | 1959 | screened | 56°01'59.16" | 12°10'31.30" | 2,413     |
| 32 | Margretheholm-1 | 2003 | screened | 55°41'21.24" | 12°38'00.72" | 2,210     |
| 33 | Margretheholm-2 | 2004 | screened | 55°41'23.17" | 12°38'04.98" | 3,290     |
| 34 | Slagelse-1      | 1959 | screened | 55°22'21.84" | 11°22'41.32" | 2,934     |
| 35 | Stenlille-2     | n.a. | screened | 55°32'17.33" | 11°36'39.17" | n.a.      |
| 36 | Stenlille-3     | n.a. | screened | 55°32'17.00" | 11°36'18.00" | n.a.      |
| 37 | Stenlille-4     | n.a. | screened | 55°31'06.47" | 11°35'13.70" | n.a.      |
| 38 | Stenlille-5     | n.a. | screened | 55°32'08.25" | 11°37'33.24" | n.a.      |
| 39 | Stenlille-6     | n.a. | screened | 55°33'28.75" | 11°39'08.52" | n.a.      |
| 40 | Stenlille-7     | n.a. | screened | 55°32'18.00" | 11°36'27.00" | n.a.      |
| 41 | Stenlille-8     | n.a. | screened | 55°32'18.94" | 11°36'25.82" | n.a.      |
| 42 | Stenlille-9     | n.a. | screened | 55°32'17.98" | 11°36'25.54" | n.a.      |
| 43 | Stenlille-10    | n.a. | screened | 55°33'00.13" | 11°35'58.77" | n.a.      |
| 44 | Stenlille-11    | n.a. | screened | 55°32'19.10" | 11°36'24.10" | n.a.      |
| 45 | Stenlille-12    | n.a. | screened | 55°32'18.29" | 11°36'22.16" | n.a.      |
| 46 | Stenlille-13    | n.a. | screened | 55°32'18.40" | 11°36'20.40" | n.a.      |
| 47 | Stenlille-14    | n.a. | screened | 55°32'19.25" | 11°36'22.44" | n.a.      |
| 48 | Stenlille-15    | n.a. | screened | 55°30'41.78" | 11°33'56.05" | n.a.      |
| 49 | Stenlille-16    | n.a. | screened | 55°32'19.41" | 11°36'20.75" | n.a.      |
| 50 | Stenlille-17    | n.a. | screened | 55°32'01.93" | 11°35'55.96" | n.a.      |
| 51 | Stenlille-18    | n.a. | screened | 55°32'02.30" | 11°35'54.38" | n.a.      |
| 52 | Thisted-1       | 1967 | screened | 57°01'26.00" | 08°39'10.00" | 909       |
| 53 | Thisted-3       | 1983 | screened | 56°57'59.22" | 08°44'25.76" | 1,208     |
| 54 | Uglev-1         | 1951 | screened | 56°37'34.80" | 08°32'08.80" | 1,208     |
| 55 | Vemb-1          | 1958 | screened | 56°22'53.40" | 08°21'46.84" | 1,944     |
| 56 | Vinding-1       | 1947 | screened | 56°17'26.00" | 08°41'56.00" | 2,372     |

and supported by the Danish Council for Strategic Research, (project#: 2104-09-0082). The author is grateful to the Geological Survey of Denmark and Greenland (GEUS) for providing the geological model of Denmark and digital background data from boreholes, logging data and core material. Project coordination by, and discussions with, Lars Henrik Nielsen, Anders Mathiesen, Rikke Weibel (all GEUS) and, for many more reasons, particularly Niels Balling (Aarhus University) are gratefully acknowledged. The authors is grateful to the three reviewers (W. Fjeldskaar; two anonymous) for their constructive comments that helped to improve the manuscript.

## References

- Balling, N., 1979. Subsurface temperatures and heat flow estimates in Denmark. In: Čermák, V., Rybach, L. (Eds.), *Terrestrial Heat Flow in Europe*. Springer, Berlin Heidelberg, pp. 161–171. [http://dx.doi.org/10.1007/978-3-642-95357-6\\_15](http://dx.doi.org/10.1007/978-3-642-95357-6_15).
- Balling, N., 1986. Temperature of geothermal reservoirs in Denmark. Report to Commission of the European Communities (EG-A-1-032-DK(G)). University of Aarhus, Geophysical Laboratory, Aarhus, Denmark, pp. 72.
- Balling, N., 2013. The Lithosphere Beneath Northern Europe: Structure and Evolution Over Three Billion Years – Contributions from Geophysical Studies, Thesis. Aarhus University, Aarhus, Denmark.
- Balling, N., Kristiansen, J.I., Breiner, N., Poulsen, K.D., Rasmussen, R., Saxov, S., 1981. Geothermal measurements and subsurface temperature modelling in Denmark. *Geologiske Skrifter* 16, 172.
- Balling, N., Nielsen, S.B., Christiansen, L.D., Poulsen, S., 1992. The Subsurface Thermal Regime and Temperature of Geothermal Reservoirs in Denmark. Research Report. University of Aarhus, Department of Earth Sciences, Aarhus, Denmark, pp. 91.
- Balling, N., Poulsen, S.E., Fuchs, S., Mathiesen, A., Bording, T.S., Nielsen, S.B., Nielsen, L.H., 2016. Development of a numerical 3D geothermal model for Denmark. *Strasbourg, Proc European Geothermal Congress 2016*, pp. 19–24.
- Bergerat, F., Angelier, J., Andreasson, P.-G., 2007. Evolution of paleostress fields and brittle deformation of the Tornquist Zone in Scania (Sweden) during Permo-Mesozoic and Cenozoic times. *Tectonophysics* 444, 93–110. <http://dx.doi.org/10.1016/j.tecto.2007.08.005>.
- Bergström, J., 1984. Lateral movements in the Tornquist Zone. *Geologiska Föreningens i Stockholm Förhandlingar* 106, 379–380.
- Bertelsen, F., 1978. The upper Triassic – lower Jurassic Vinding and Gassum formations of the Norwegian-Danish basin. *Danmarks Geologiske Undersøgelse Serie B*, vol. 3 26 pp.
- Bertelsen, F., 1980. Lithostratigraphy and depositional history of the Danish Triassic. *Danmarks Geologiske Undersøgelse Serie B*, vol. 4 59 pp.
- Blackwell, D.D., Steele, J.L., 1989. Thermal conductivity of sedimentary rocks; measurement and significance. In: Naeser, N.D., McCulloh, T.H. (Eds.), *Thermal History of Sedimentary Basins; Methods and Case Histories*. Springer, Berlin, pp. 13–36. [http://dx.doi.org/10.1007/978-1-4612-3492-0\\_2](http://dx.doi.org/10.1007/978-1-4612-3492-0_2).
- Bücker, C., Rybach, L., 1996. A simple method to determine heat production from gamma-ray logs. *Mar. Petrol. Geol.* 13 (4), 373–375. [http://dx.doi.org/10.1016/0264-8172\(95\)00089-5](http://dx.doi.org/10.1016/0264-8172(95)00089-5).
- Chapman, D.S., Keho, T., Bauer, M., Picard, M., 1984. Heat flow in the Uinta Basin determined from bottom hole temperature (BHT) data. *Geophysics* 49, 453–466. <http://dx.doi.org/10.1190/1.1441680>.
- Clavier, C., Hoyle, W., Meunier, D., 1971. Quantitative interpretation of thermal neutron decay time logs: part I. Fundamentals and techniques. *J. Pet. Technol.* 23, 743–755. <http://dx.doi.org/10.2118/2658-A-PA>.
- Deming, D., Nunn, J.A., Jones, S., Chapman, D.S., 1990. Some problems in thermal history studies. In: Nuccio, V.F., Barker, C.E., Dyson, S.J. (Eds.), *Applications of Thermal Maturity Studies to Energy Exploration, MS-SEPM*, pp. 61–80.
- Deutsch, C.V., Journel, A.G., 1998. *Gslib: Geostatistical software Library and User's Guide*. Oxford University Press, Incorporated, New York 369 p.
- Eugeno-S Working Group, 1988. Crustal structure and tectonic evolution of the transition between the Baltic Shield and the North German Caledonides (the EUGENO-S Project). *Tectonophysics* 150, 253–348. [http://dx.doi.org/10.1016/0040-1951\(88\)90073-X](http://dx.doi.org/10.1016/0040-1951(88)90073-X).
- Fjeldskaar, W., Amantov, A., 2017. Effects of glaciations on sedimentary basins. *J. Geodynamic* 118, 66–81. <http://dx.doi.org/10.1016/j.jog.2017.10.005>.
- Fjeldskaar, W., Prestholm, E., Guargena, C., Stephenson, M., et al., 1993. Mineralogical and diagenetic control on the thermal conductivity of the sedimentary sequences in the Bjørnøya Basin, Barents Sea. In: Doré, T. (Ed.), *Basin Modelling: Advances and Applications*. Elsevier, Amsterdam, pp. 445–453.
- Fjeldskaar, W., Helset, H.M., Johansen, H., Grunnaleite, I., Horstad, I., 2008. Thermal modelling of magmatic intrusions in the Gjallar Ridge, Norwegian Sea: implications for vitrinite reflectance and hydrocarbon maturation. *Basin Res.* 20, p143–159. <http://dx.doi.org/10.1111/j.1365-2117.2007.00347.x>.
- Frederiksen, S., Nielsen, S.B., Balling, N., 2001. A numerical dynamic model for the Norwegian-Danish Basin. *Tectonophysics* 343, 165–183. [http://dx.doi.org/10.1016/S0040-1951\(01\)00223-2](http://dx.doi.org/10.1016/S0040-1951(01)00223-2).
- Fuchs, S., Balling, N., 2016a. Improving the temperature predictions of subsurface thermal models by using high-quality input data. Part 1: uncertainty analysis of the thermal-conductivity parameterization. *Geothermics* 64, 42–54. <http://dx.doi.org/10.1016/j.geothermics.2016.04.010>.
- Fuchs, S., Balling, N., 2016b. Improving the temperature predictions of thermal models by using high-quality input data. Part 2: a case study from the Danish-German border region. *Geothermics* 64, 1–14. <http://dx.doi.org/10.1016/j.geothermics.2016.04.004>.
- Fuchs, S., Förster, A., 2010. Rock thermal conductivity of Mesozoic geothermal aquifers in the Northeast German Basin. *Chem. Erde-Geochem.* 70, 13–22. <http://dx.doi.org/10.1016/j.chemer.2010.05.010>.
- Fuchs, S., Förster, A., 2014. Well-log based prediction of thermal conductivity of sedimentary successions: a case study from the North German Basin. *Geophys. J. Int.* 196, 291–311. <http://dx.doi.org/10.1093/gji/ggt382>.
- Fuchs, S., Balling, N., Förster, A., 2015. Calculation of thermal conductivity, thermal diffusivity and specific heat capacity of sedimentary rocks using petrophysical well logs. *Geophys. J. Int.* 203, 1977–2000. <http://dx.doi.org/10.1093/gji/ggv403>.
- Gallardo, J., Blackwell, D.D., 1999. Thermal structure of the Anadarko basin. *AAPG Bull.* 83, 333–361.
- Götz, A.E., Török, Á., Sass, I., 2014. Geothermal reservoir characteristics of Meso- and Cenozoic sedimentary rocks of Budapest (Hungary). *Zeitschrift der Deutschen Gesellschaft für Geowissenschaften* 165, 487–493. <http://dx.doi.org/10.1127/1860-1804/2014/0069>.
- Hamberg, L., Nielsen, L.H., 2000. Shingled, Sharp Based Shoreface Sandstone: Depositional Response to Stepwise Forced Regression in a Shallow Basin, Upper Triassic Gassum Formation, Denmark, vol. 172. Geological Society, London, pp. 69–89. <http://dx.doi.org/10.1144/gsl.sp.2000.172.01.04>. Special Publication.
- Homuth, S., Götz, A.E., Sass, I., 2014. Lithofacies and depth dependency of thermo- and petrophysical rock parameters of the Upper Jurassic geothermal carbonate reservoirs of the Molasse Basin. *Zeitschrift der Deutschen Gesellschaft für Geowissenschaften*. 165, 469–486. <http://dx.doi.org/10.1127/1860-1804/2014/0074>.
- Mathiesen, A., Kristensen, L., Bidstrup, T., Nielsen, L.H., 2009. Vurdering af det geotermiske potentiale i Danmark. *Danmarks Grønlands Geologiske Undersøgelse Rapport*. GEUS 85 pp.
- Mathiesen, A., Nielsen, L.H., Bidstrup, T., 2010. Identifying potential geothermal reservoirs in Denmark. *Geol. Surv. Den. Greenl. Bull.* 20, 19–22.
- Michelsen, O., 1978. Stratigraphy and Distribution of Jurassic Deposits of the Norwegian-Danish Basin. *Danmarks geologiske undersøgelse B2*, 28 pp.
- Michelsen, O., Clausen, O.R., 2002. Detailed stratigraphic subdivision and regional correlation of the southern Danish Triassic succession. *Mar. Petrol. Geol.* 19, 563–587. [http://dx.doi.org/10.1016/S0264-8172\(02\)00028-4](http://dx.doi.org/10.1016/S0264-8172(02)00028-4).
- Michelsen, O., Nielsen, L.H., Johannessen, P.N., Andsjberg, J., Surlyk, F., 2003. Jurassic lithostratigraphy and stratigraphic development onshore and offshore Denmark. In: Ineson, J.R., Surlyk, F. (Eds.), *The Jurassic of Denmark and Greenland, Geological Survey of Denmark and Greenland Bulletin*, vol. 1. GEUS, pp. 147–216.
- Mottaghy, D., Pechnig, R., Vogt, C., 2011. The geothermal project Den Haag: 3D numerical models for temperature prediction and reservoir simulation. *Geothermics* 40, 199–210. <http://dx.doi.org/10.1016/j.geothermics.2011.07.001>.
- Nielsen, L.H., 2003. Late Triassic–Jurassic development of the Danish Basin and the Fennoscandian Border Zone, southern Scandinavia. In: Ineson, J.R., Surlyk, F. (Eds.), *The Jurassic of Denmark and Greenland, Geological Survey of Denmark and Greenland Bulletin*, vol. 1. GEUS, pp. 459–526.
- Nielsen, L.H., Mathiesen, A., Bidstrup, T., 2004. Geothermal energy in Denmark. *Geol. Surv. Den. Greenl. Bull.* 4, 17–20.
- Norden, B., Förster, A., 2006. Thermal conductivity and radiogenic heat production of sedimentary and magmatic rocks in the Northeast German Basin. *AAPG Bull.* 90, 939–962. <http://dx.doi.org/10.1306/01250605100>.
- Norden, B., Förster, A., Behrends, K., Krause, K., Stecken, L., Meyer, R., 2012. Geological 3-D model of the larger Altensalzwedel area, Germany, for temperature prognosis and reservoir simulation. *Environ. Earth Sci.* 67, 511–526. <http://dx.doi.org/10.1007/s12665-012-1709-9>.
- Poulsen, S.E., Balling, N., Bording, T.S., Mathiesen, A., Nielsen, S.B., 2017. Inverse geothermal modelling applied to Danish sedimentary basins. *Geophys. J. Int.* 211, 188–206. <http://dx.doi.org/10.1093/gji/ggx296>.
- Powell, W.G., Chapman, D.S., 1990. A detailed study of heat flow at the Fifth Water Site, Utah, in the Basin and Range-Colorado Plateaus transition. *Tectonophysics* 176, 291–314. [http://dx.doi.org/10.1016/0040-1951\(90\)90075-J](http://dx.doi.org/10.1016/0040-1951(90)90075-J).
- Raymer, L.L., Hunt, E.R., Gardner, J.S., 1980. An improved sonic transit time-to-porosity transform. In: *SPWLA 21st Annual Logging Symposium*, Lafayette, Louisiana, USA.
- Rybach, L., 1986. Amount and significance of radioactive heat sources in sediments. In: Burrus, J. (Ed.), *Thermal Modelling in Sedimentary Basins: 1st IFP Exploration Research Conference Carcans, Editions Technip. Carcans, France*, pp. 311–322.
- Schön, J.H., 2011. *Physical Properties of Rocks: A Workbook*. Elsevier.
- Schütz, F., Fuchs, S., Förster, A., 2012a. Thermal conductivity of sedimentary rocks: the significance of facies-related trends. In: *Geothermiekongress 2012*. Karlsruhe, Germany.
- Schütz, F., Norden, B., Förster, A., Group, Desire, 2012b. Thermal properties of sediments in southern Israel: a comprehensive data set for heat flow and geothermal energy studies. *Basin Res.* 24, 357–376. <http://dx.doi.org/10.1111/j.1365-2117.2011.00529.x>.
- Schütz, F., Fuchs, S., Förster, A., Förster, H.-J., 2013. Facies-related trends of rock thermal conductivity and the impact on temperature prognosis for geothermal target reservoirs. In: *General Assembly European Geosciences Union, Geophysical Research Abstracts*. Vienna, Austria.
- Serra, O., 1986. *Fundamentals of Well-Log Interpretation – The Interpretation of Logging Data*. Elsevier, Amsterdam - Oxford - New York - Tokyo.
- Sippel, J., Fuchs, S., Cacace, M., Braatz, A., Kastner, O., Huenges, E., Scheck-Wenderoth, M., 2013. Deep 3D thermal modelling for the city of Berlin (Germany). *Environ. Earth Sci.* 70, 3545–3566. <http://dx.doi.org/10.1007/s12665-013-2679-2>.
- Sorgenfrei, T., Buch, A., 1964. *Deep Tests in Denmark*, Geological Survey of Denmark. Copenhagen, Denmark.
- Theys, P., 1999. *Log Data Acquisition and Quality Control*. Edition Technip, Paris.
- Thybo, H., 1997. Geophysical characteristics of the Tornquist Fan area, northwest Trans-European Suture Zone: indication of late Carboniferous to early Permian dextral Transtension. *Geol. Mag.* 134, 597–606. <http://dx.doi.org/10.1017/>

- S0016756897007267.
- Thybo, H., 2001. Crustal structure along the EGT profile across the Tornquist Fan interpreted from seismic, gravity and magnetic data. *Tectonophysics* 334, 155–190. [http://dx.doi.org/10.1016/S0040-1951\(01\)00055-5](http://dx.doi.org/10.1016/S0040-1951(01)00055-5).
- Vejbæk, O.V., 1989. Effects of asthenospheric heat flow in basin modelling exemplified with the Danish Basin. *Earth. Planet. Sci. Lett.* 95, 97–114. [http://dx.doi.org/10.1016/0012-821X\(89\)90170-2](http://dx.doi.org/10.1016/0012-821X(89)90170-2).
- Vilà, M., Fernández, M., Jiménez-Munt, I., 2010. Radiogenic heat production variability of some common lithological groups and its significance to lithospheric thermal modeling. *Tectonophysics* 490, 152–164. <http://dx.doi.org/10.1016/j.tecto.2010.05.003>.
- Vogt, C., Mottaghy, D., Wolf, A., Rath, V., Pechinig, R., Clauser, C., 2010. Reducing temperature uncertainties by stochastic geothermal reservoir modelling. *Geophys. J. Int.* 181, 321–333. <http://dx.doi.org/10.1111/j.1365-246X.2009.04498.x>.
- Weibel, R., Kjøller, C., Bateman, K., Nielsen, L.H., Frykman, P., Springer, N., Laier, T., 2011. Mineral changes in CO<sub>2</sub> experiments — examples from Danish onshore saline aquifers. *Energy Procedia* 4, 4495–4502. <http://dx.doi.org/10.1016/j.egypro.2011.02.405>.
- Weibel, R., Olivarius, M., Kristensen, L., Friis, H., Hjuler, M.L., Kjøller, C., Mathiesen, A., Nielsen, L.H., 2017. Predicting permeability of low-enthalpy geothermal reservoirs: a case study from the Upper Triassic–Lower Jurassic Gassum Formation, Norwegian–Danish Basin. *Geothermics* 65, 135–157. <http://dx.doi.org/10.1016/j.geothermics.2016.09.003>.
- Wyllie, M.R.J., Gregory, A.R., Gardner, G.H.F., 1958. An experimental investigation of factors affecting elastic wave velocities in porous media. *Geophysics* 23, 459–493. <http://dx.doi.org/10.1190/1.1438493>.
- Ziegler, P.A., 2005. Europe: Permian to recent evolution. In: Selley, R.C., Cocks, L.R.M., Plimer, I.R. (Eds.), *Encyclopedia of Geology*. Elsevier, pp. 102–125.